



Biomass into chemicals: One-pot two- and three-step synthesis of quinoxalines from biomass-derived glycols and 1,2-dinitrobenzene derivatives using supported gold nanoparticles as catalysts

M.J. Climent ^a, A. Corma ^{a,*}, J.C. Hernández ^b, A.B. Hungría ^b, S. Iborra ^{a,*}, S. Martínez-Silvestre ^a

^a Instituto de Tecnología Química (UPV-CSIC), Universitat Politècnica de Valencia, Consejo Superior de Investigaciones Científicas, Avenida de los Naranjos s/n, 46022 Valencia, Spain

^b Departamento de Ciencia de los Materiales e Ingeniería Metalúrgica y Química Inorgánica, Universidad de Cádiz (UCA), Carpas Río San Pedro s/n, 11510 Puerto Real, Cádiz, Spain

ARTICLE INFO

Article history:

Received 27 March 2012

Revised 30 April 2012

Accepted 2 May 2012

Available online 7 June 2012

Keywords:

Cascade process

Quinoxaline

2-Methylquinoxaline

Au/CeO₂

Au/HT

Heterogeneous catalyst

1,2-Phenylenediamine

Diol

Biomass

ABSTRACT

An efficient and selective one-pot two-step method, for the synthesis of quinoxalines by oxidative coupling of vicinal diols with 1,2-phenylenediamine derivatives, has been developed by using gold nanoparticles supported on nanoparticulated ceria (Au/CeO₂) or hydrotalcite (Au/HT) as catalysts and air as oxidant, in the absence of any homogeneous base. Reaction kinetics shows that the reaction controlling step is the oxidation of the diol to α -hydroxycarbonyl compound. Furthermore, a one-pot three-step synthesis of 2-methylquinoxaline starting from 1,2-dinitrobenzene and 1,2-propanediol has been successfully carried out with 98% conversion and 83% global yield to the final product.

© 2012 Elsevier Inc. All rights reserved.

1. Introduction

In the last decade, the research of renewable reactants has become a key issue for a sustainable chemistry [1–5]. Approximately 75% of the biomass produced by nature through the process of photosynthesis corresponds to carbohydrates, but only between 3% and 4% of these compounds are used for food and non-food purposes [6]. Therefore, the use of carbohydrates as raw materials for the production of basic chemicals is an area of increasing interests [7–11]. In this sense, a variety of glycols (1,2-ethanediol, 1,2-propanediol, 1,2-butanediol, or 2,3-butanediol) can be obtained from carbohydrates [1–5,12] as well as from glycerol [13,14] via bio- or chemocatalytic reactions. Those glycols could be used as starting reactants to obtain products with higher added value.

The aim of the present work is to obtain quinoxalines starting from glycols derived from biomass and 1,2-phenylenediamine or 1,2-dinitrobenzene derivatives, through a cascade reaction process. Quinoxalines, also called benzopyrazines, and their derivatives show a broad spectrum of biological activity, including antitumor [15], antiviral [16], antituberculosis [17], anti-inflammatory

[18,19], anti-protozoal, and anti-HIV [20,21], and have been evaluated as anticancer and anthelmintic agents [22]. Quinoxaline moieties have also found applications as dyes [23], cavitands [24], efficient electroluminescent materials [25], building blocks in the synthesis of organic semiconductors [26], chemically controllable switches [27], and dehydroannulenes [28].

Quinoxaline synthesis is conventionally carried out by a double condensation between 1,2-phenylenediamines and 1,2-dicarbonyl compounds [29–33]. However, the handling of highly reactive dicarbonyl compounds is an important drawback. Other synthesis methods involving 1,4-addition of 1,2-diamines to diazenylbutenes [34], oxidation trapping of α -hydroxycarbonyl compounds with 1,2-diamines [35–38], cyclization–oxidation of phenacyl bromides and 1,2-phenylenediamines through solid-phase synthesis [39], and oxidative coupling of epoxides with ene-1,2-diamines [40] have been developed for the synthesis of substituted quinoxalines. Unfortunately, most of these methods suffer from unsatisfactory yields, difficult experimental procedures, the use of expensive and detrimental metal precursors, or demanding reaction conditions. Therefore, there is a clear incentive to develop catalytic process able to produce the quinoxalines by environmentally friendly methods, while minimizing the number of reaction steps through a more intensive one pot–type catalytic process.

* Corresponding authors. Fax: +34 963877809 (A. Corma).

E-mail addresses: acorma@itq.upv.es (A. Corma), siborra@itq.upv.es (S. Iborra).

chemical analysis. The metal particle size was determined by High Angle Annular Dark Field Scanning Transmission Electron Microscopy (HAADF-STEM), and images were acquired with a JEOL 2010 field emission gun transmission electron microscope operated at 200 kV equipped with a X-EDS Oxford Inca Energy 2000 system.

2.1.2. Synthesis of Au/HT catalysts

The Al/Mg hydrotalcite (HT) support was prepared by co-precipitation of two salts containing Al^{3+} and Mg^{2+} [53]. The synthesis is performed at constant pH, by slow addition, in a single container, of two diluted solutions (A and B), namely solution A containing $\text{Mg}(\text{NO}_3)_2 \cdot 6\text{H}_2\text{O}$ and $\text{Al}(\text{NO}_3)_3 \cdot 9\text{H}_2\text{O}$, 1.5 M in (Al + Mg) with Al/(Al + Mg) atomic ratio equal to 0.25, and solution B prepared by dissolving Na_2CO_3 and NaOH in water in such a way that the ratio $\text{CO}_3^{2-}/(\text{Al} + \text{Mg})$ is equal to 0.66. Both solutions were co-added at a rate of 1 mL min^{-1} under vigorous mechanical stirring at room temperature. The gel was aged under autogeneous pressure conditions at 333 K for 12 h. Then, the hydrotalcite was filtered and washed until $\text{pH} = 7$ and the solid was dried.

To prepare an Au/HT catalyst, the obtained HT (1.0 g) was added to 50 mL of an aqueous solution of HAuCl_4 (2 mM). After stirring for 2 min, 0.09 mL of aqueous NH_3 (10% v/v) was added and the resulting mixture stirred at room temperature for 12 h. The obtained slurry was filtered, washed with deionized water, and dried at room temperature in vacuo. Subsequent treatment with H_2 (flow = 90 mL min^{-1}) at 180°C for 3 h gives Au/HT sample as a purplish red powder. The Au loading on Au/HT was found to be 0.7 wt% by elemental analysis. Another catalyst was prepared where the original HT support was calcined at 450°C in a N_2 flow for 6 h to produce the mixed oxides before 0.7 wt% gold was supported following the same procedure than above. The resultant catalyst is named Au/HTcalc.

2.1.3. Synthesis of Au/MgO catalyst

A nanocrystalline MgO support ($\geq 600 \text{ m}^2 \text{ g}^{-1}$ BET surface area) was purchased from NanoScale Materials Inc. The synthesis of Au/MgO sample was carried out from MgO and an aqueous solution of HAuCl_4 , following the method described for Au/HT. Chemical analysis gave 0.6 wt% Au on the catalyst.

2.1.4. 1.5 wt% Au/ TiO_2 and 4.5 wt% Au/ Fe_2O_3 catalysts

These samples were directly purchased from TEK and WGC, respectively, and they were used as received.

2.2. Reagents

All reagents were purchased from Sigma Aldrich except $\text{Au}(\text{CH}_3)_2(\text{acac})$ which was purchased from Strem, and 4-methoxybenzene-1,2-diamine which was synthesized from 4-methoxy-2-nitroaniline by hydrogenation of the nitro group over Au/ TiO_2 [54].

2.3. Catalyst regeneration and reuse

For catalyst reuse, the catalyst after reaction was collected by vacuum filtration, and then it was repeatedly washed. First, it was washed with diethyl ether to remove organic compounds; subsequently, it was washed with NaOH (0.2 mol L^{-1}) to remove any acid by-products that may poison the gold nanoparticles. Then, water was used to remove traces of NaOH on the catalyst, and at last the catalyst was washed with diethyl ether again. Finally, the catalyst was dried overnight, and then it is ready for reuse.

2.4. Reaction procedure

A generic experiment was as follows. In a two-neck round-bottom flask of 10 mL, 1,2-phenylenediamine (**1a**, 0.5 mmol),

1,2-propyleneglycol (**2a**, 0.6 mmol), 1.5 mL of diethylene glycol dimethyl ether (diglyme), and an amount of catalyst were added. Subsequently, the reaction mixture was heated at 140°C in a silicone bath that contains a magnetic stirrer and a temperature controller. In another series of experiments, the same methodology was followed, but some of the reaction conditions were changed in order to see the effect of temperature, diamine/Au ratio, catalyst loading, and oxygen pressure.

For the one-pot three-step experiment, the reaction was performed using 0.5 mmol of 1,2-dinitrobenzene, 0.6 mmol of **2a**, 10.5 mmol of diglyme, and 20 mg of Au/ CeO_2 (4.5 wt%) as catalyst.

The progress of the reaction was followed by taking samples at regular time periods and analyzing them by gas chromatography using a FID detector and a capillary column (HP5, $30 \text{ m} \times 0.25 \text{ mm} \times 0.25 \mu\text{m}$). All samples were dissolved in ethyl acetate prior to analysis by gas chromatography. Nitrobenzene was used as the external standard. At the end of the reaction, the catalyst was filtered and washed according to the regeneration of the catalyst section. The extract is concentrated and quantified in the final outcome of the reaction, and the catalyst is ready to be reused. In all cases, the total final mass of the reaction (including the filtered extract) was over 90% of the initial amount weighed.

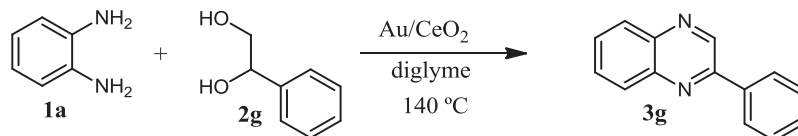
The products obtained were characterized by ^1H -RMN (300 MHz Bruker Avance). The content of organic (wt% C, H, N, S) was measured by elemental analysis with an EA-1108 CHNS Fisons analyzer and sulfanilamide as standard. The thermogravimetric analyses were carried out with a TGA 2050 by TA Instruments, under an air flow, and with a heating rate of 10 K min^{-1} . Mass spectra were recorded by GC-MS (HP Agilent 5988 A with a 6980 mass selective detector).

3. Results and discussion

3.1. Reaction network

Following the general reaction procedure previously explained and using Au/ CeO_2 as catalyst, the reaction between 1,2-phenylenediamine (**1a**) and 1-phenylethane-1,2-diol (**2g**) (Scheme 3) was followed with time, and the kinetic curves are given in Fig. 1 (see also Scheme 4). At the beginning of the reaction, only the α -hydroxycarbonyl compound (**4**), formed by oxidation of the diol **2g**, and benzaldehyde (**6**) that comes from the oxidative cleavage of **2g** were observed as primary products. However, after 1-h reaction, their concentration decreases probably by reaction of the α -hydroxycarbonyl compound (**4**) with a molecule of phenylenediamine **1a** to afford 2-phenylquinoxaline **3** and, in a much lesser degree, the benzimidazole derivatives (**8**, **9**, **10**, and **11**) [55]. Since this consecutive reaction is very fast, product **3** appears as a pseudo primary product. The dicarbonyl compound (**5**), produced by oxidation of α -hydroxycarbonyl compound **4**, was detected at trace level, and the formaldehyde (**7**) produced by oxidative cleavage of the diol was not detected. This behavior allows us to consider that the α -hydroxycarbonyl compound **4** is a primary and unstable product and dicarbonyl compound **5** is a secondary and unstable product.

Taking into account the kinetic behavior of the different compounds presented in Fig. 1, a reaction network is presented in Scheme 5, where the diol **2** is firstly oxidized to the α -hydroxycarbonyl compound **4** and subsequently to the dicarbonyl compound **5**. Both compounds can condensate with the diamine **1** to produce the imine intermediates **13** and **14** (non-detectable by GC), being **13** converted into product **14** by a fast oxidation of the remaining hydroxyl group. Finally, product **14** follows the condensation to yield quinoxaline **3**. Additionally, we have reacted 2-hydroxy-1-phenylethanone **4** and 2-oxo-2-phenylacetaldehyde **5** under the



Scheme 3. Reaction pathway for the oxidation–cyclization reaction of **1a** with **2g** using Au/CeO₂. Reaction conditions: **1a** (0.5 mmol), **2g** (0.6 mmol), diglyme (10.5 mmol), Au/CeO₂ (2.4 wt%), **1a**/Au mol ratio = 100, at 140 °C.

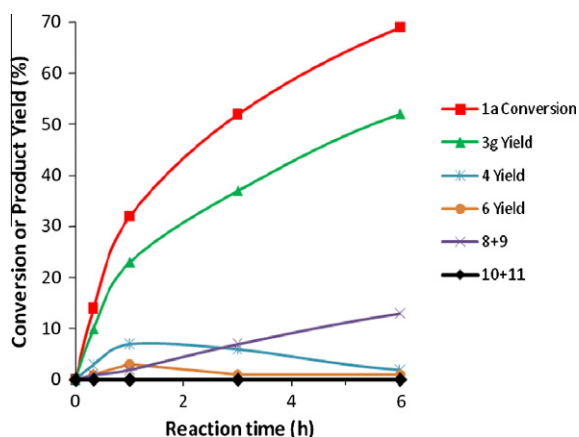


Fig. 1. Kinetic plots of the different compounds (mol%) detected in the oxidation–cyclization reaction of **1a** with **2g** using Au/CeO₂. Reaction conditions: **1a** (0.5 mmol), **2g** (0.6 mmol), diglyme (10.5 mmol), Au/CeO₂ (4.5 wt%), **1a**/Au mol ratio = 100, at 140 °C.

same reaction conditions. Then, from the results given in Table 1, one can see that when starting from **2g**, the reaction is slower than when the reaction started from α -hydroxycarbonyl compound **4**. Moreover, when we fed dicarbonyl compound **5**, the reaction was very fast. From these results, we can conclude that the controlling reaction step in the process should be the oxidation of compound **2** into compound **4**.

Interestingly, we found that when the reaction started from diol **2g** or α -hydroxycarbonyl compound **4**, the same type of by-products (**6**, **8**, and **9**) were detected, while in the experiment starting with dicarbonyl compound **5**, no by-products were observed. These results show that the by-products detected are produced from the oxidative cleavage of the diol and/or the hydroxycarbonyl compound **4** into the aldehydes **6** and **7**. Later, products **6** and **7** condensate with phenylenediamine **1** giving the benzimidazole derivatives **8**, **9**, **10**, and **11**.

3.2. Reactivity of the different metal-supported catalysts

In order to determine the possibilities of gold as a catalyst for the synthesis of quinoxalines, the catalytic activity of different

gold-supported catalysts was studied for the reaction of 1,2-phenylenediamine (**1a**) with the 1,2-propanediol (**2a**) to obtain 2-methylquinoxaline (**3a**) (Scheme 6). Thus, the reaction was carried out in diglyme as a solvent at 140 °C in the presence of gold supported on: CeO₂ nanoparticles, TiO₂, Fe₂O₃, MgO, HT, and calcined HT (HTcalc). Regardless of the support used, gold was active and selective for the aforementioned reaction (Table 2) and, in all cases, the main by-products detected were 2-methyl-1H-benzo[d]imidazole (**8**) and 1-H-benzo[d]imidazole (**9**), which are produced from the oxidative cleavage of 1,2-propanediol giving the corresponding aldehydes, followed by condensation with 1,2-phenylenediamine (see Scheme 5).

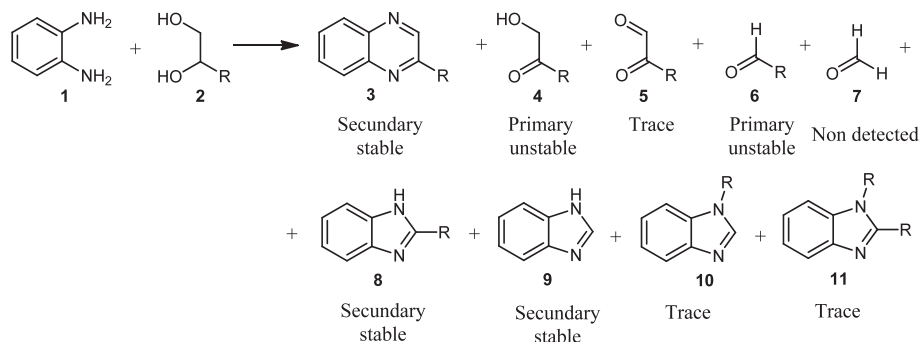
In a first approximation, we have checked whether the differences in activity observed among the different catalysts can be due to difference in metal particle size. Then, the number of external surface atoms was calculated for each catalyst on the basis of the mean particle size, and with this value and initial reaction rates, a turnover frequency (TOF) was calculated for each catalyst. According to the TEM images, the shape of gold nanoparticles looks predominantly cubic. Thus, by assuming this crystal shape, the number of particle gold atoms (N_T) was calculated according to Eq. (1), in which $\langle d \rangle$ corresponds to the mean diameter of gold particles as determined experimentally by TEM and d_{at} is the atomic diameter of gold (0.288 nm). Considering that in the face-centered cubic (fcc) crystal one atom is surrounded by 12 others assuming a full shell close packing model and N_T is related to the number of shells (m) [Eq. (2)], then the number of external atoms (N_S) can be calculated with Eq. (3) [56,57].

$$N_T = \frac{10m^3 - 15m^2 + 11m - 3}{3} \quad (1)$$

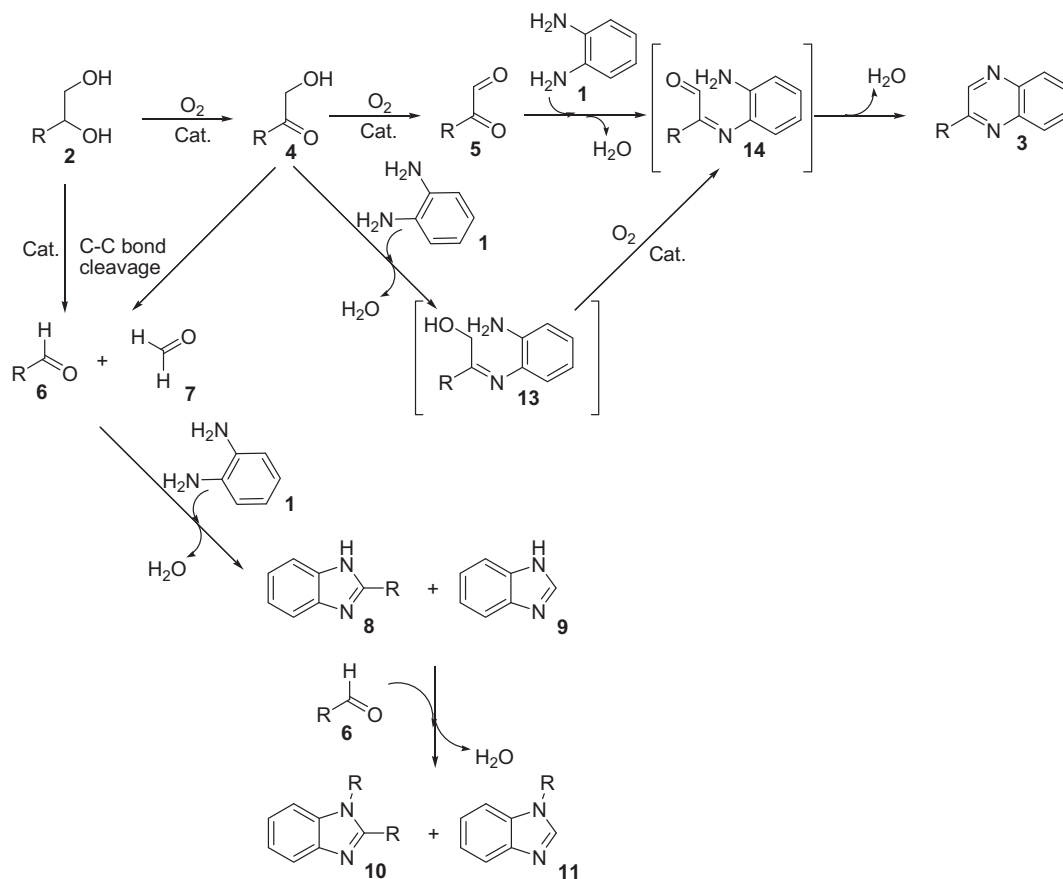
$$\langle d \rangle = 1.105 \cdot d_{at} \cdot \sqrt[3]{N_T} \quad (2)$$

$$N_S = 10m^2 - 20m + 12 \quad (3)$$

As can be seen in Table 2 and Fig. 2, Au/CeO₂ and Au/HT catalysts present the highest activity (TOF values) among the different gold catalysts tested, achieving conversions >85% with high selectivities (entries 1 and 2). Meanwhile, Au/TiO₂, Au/Fe₂O₃, and Au/MgO catalysts (entries 3, 4, and 5), which are active for different oxidation and reduction reaction, show much lower activity at a similar



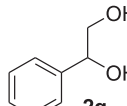
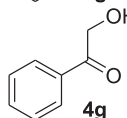
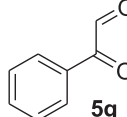
Scheme 4. Detected products in the synthesis of quinoxalines from 1,2-phenylenediamine derivatives and vicinal diols.



Scheme 5. Proposed quinoxaline synthesis mechanism from 1,2-phenylenediamine derivatives and vicinal diols.

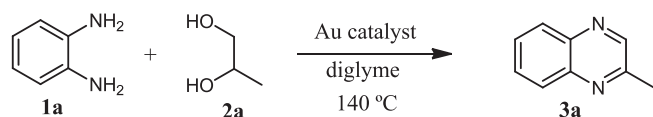
Table 1

Catalytic activity of Au/CeO₂ toward **3g** formation starting from **2g**, 2-hydroxy-1-phenylethanone (**4g**), and 2-oxo-2-phenyl-acetaldehyde (**5g**).^a

Entry	Reactant	Time (h)	Conversion (mol%)	Selectivity to 3g ^b (mol%)
1	 2g	24	97	72
		2	42	75
2	 4g	2	>99	93
3	 5g	5 (min)	>99	99

^a Reaction conditions: **1a** (0.5 mmol), **2g**(**4g** or **5g**) (0.6 mmol), diglyme (10.5 mmol), Au/CeO₂ (4.5 wt%), **1a**/Au mol ratio = 100, at 140 °C.

^b As main by-products, which complete molar balance, are the following: 2-phenyl-1H-benzo[d]imidazole (**8**) and 1H-benzo[d]imidazole (**9**).



Scheme 6. Oxidation–cyclization reaction of 1,2-phenylenediamine with 1,2-propanediol over different Au catalysts.

number of gold surface atoms than Au/CeO₂ and Au/HT. The influence of the support on the rate of alcohol oxidation by gold has been

attributed to changes produced on the crystallite shape as well as to the participation of the support in the catalytic cycle [58,59]. In the case of CeO₂, it has been reported that surface saturation by O₂ is already achieved at relatively low partial pressure of O₂, as could be expected due to the excellent capacity of CeO₂ to act as an oxygen pump due to the presence of surface oxygen vacancies that arises from the small size of ceria nanoparticles [60–62]. Otherwise, HT has a structure of brucite-like layers containing octahedrally coordinated cations of Mg²⁺ and Al³⁺ as well as interlayer anions (CO₃²⁻ and OH⁻ mainly) which has been reported as an excellent

Table 2
Results of oxidation–cyclization process of **2a** with **1a** into **3a** using different catalysts.^a

Entry	Catalyst	Au loading (wt%)	Molar ratio (1a/Au)	Average size ^b (nm)	N_T (by np)	m (layers)	N_S (by np)	N_S (%)	r_0 (mmol h ⁻¹)	TOF ₁ ^c (h ⁻¹)	Conversion (mol%)	Yield (mol%)	Selectivity to 3a ^d (mol%)
1	Au/CeO ₂	4.5	102	3.5	1285	7.8	459	36	0.21	121	95	82	87
2	Au/HT	0.7	129	3.2	1016	7.2	388	38	0.19	132	86 (92) ^e	80 (85)	94
3	Au/TiO ₂	1.5	103	3.5	1330	7.8	471	35	0.04	23	39	36	92
4	Au/Fe ₂ O ₃	4.5	99	3.5	1365	7.9	479	35	0.02	12	14	13	–
5	Au/MgO	0.6	239	3.9	1840	8.7	593	32	0.02	36	20	18	–
6	Au/HTcalc ^f	0.7	127	3.6	1448	8.1	500	35	0.12	91	71	68	96
7	CeO ₂	–	–	–	–	–	–	–	0.03	–	22	18	–
8	HT	–	–	–	–	–	–	–	0.01	–	9	7	–

^aNo-nanomeric CeO₂ was used as support.

^b Reaction conditions: **1a** (0.5 mmol), **2a** (0.6 mmol), diglyme (10.5 mmol), 24 h.

^c Determined by TEM.

^d Calculated as moles of converted **1a** divided by reaction time (0.5 h) and moles of Au in the surface (N_S).

^e Selectivity values at 40% conversion. As main by-products, which complete molar balance, are the following: 2-methyl-1H-benzo[d]imidazole (**8**) and 1H-benzo[d]imidazole (**9**).

^f Result after 30 h.

^g Hydrotalcite calcined was used as a gold support.

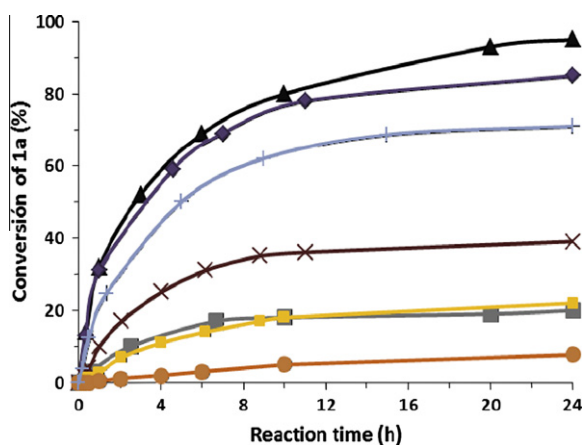


Fig. 2. Conversion kinetic plots of the oxidation–cyclization of **2a** with **1a** into **3a** using different catalysts: Au/CeO₂ (▲), Au/HT (◆), Au/HTcalc (+), Au/TiO₂ (×), Au/MgO (■), CeO₂ (■), and HT (●). Reaction conditions: **1a** (0.5 mmol), **2a** (0.6 mmol), diglyme (10.5 mmol), at 140 °C.

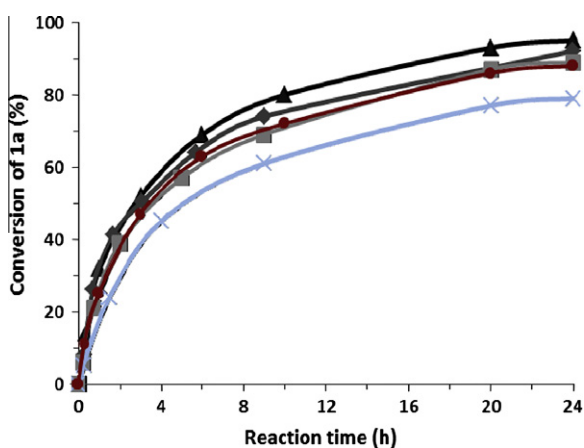


Fig. 3. Conversion kinetic plots of the oxidation–cyclization of **1a** with **2a** into **3a** under successive reuses of Au/CeO₂: 1st use (▲), 2nd use (◆), 3rd use (■), 4th use (×), and 4th use after calcination (●) treatment with air at 300 °C for 10 h. Reaction conditions: **1a** (0.5 mmol), **2a** (0.6 mmol), diglyme (10.5 mmol), at 140 °C.

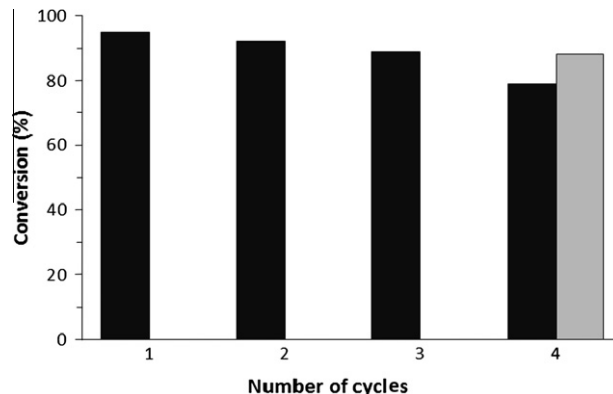


Fig. 4. Conversion of **1a** with successive reuses of Au/CeO₂ in the oxidation–cyclization of **1a** with **2a** after 24 h. In the fourth use, the bar on the right illustrates when the catalyst was used after previous treatment in air at 300 °C for 10 h. Reaction conditions: **1a** (0.5 mmol), **2a** (0.6 mmol), diglyme (10.5 mmol), Au/CeO₂ (4.5 wt%), **1a**/Au mol ratio = 100, at 140 °C.

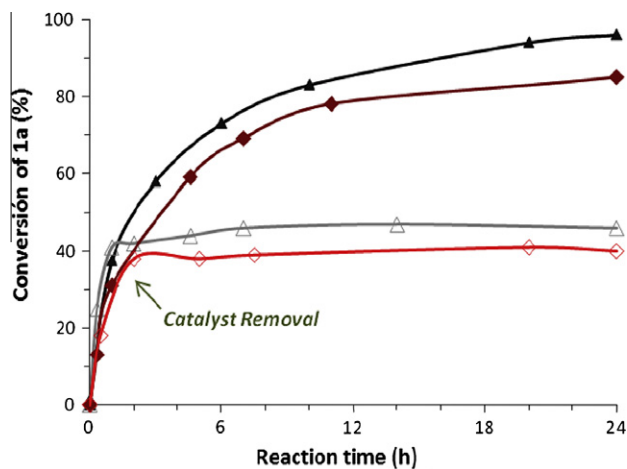


Fig. 5. Conversion kinetic plots of the **1a** in the oxidation–cyclization process of **1a** with **2a** into **3a** using Au/CeO₂ (4.5 wt%) and Au/HT (0.75 wt%). Au/CeO₂ (▲) and Au/HT (◆) are the same experiments than Au/CeO₂ (▲) and Au/HT (◆) but removing the catalyst after 2 h of reaction. Reaction conditions: **1a** (0.5 mmol), **2a** (0.6 mmol), diglyme (10.5 mmol), **1a**/Au mol ratio = 100, at 140 °C.

catalyst for alcohol oxidation that form Au-alcoholate species [63–66] due to the basic surfaces of HT. However, when HT support is calcined, the layered structure disappears and a mixed Al_2O_3 – MgO oxide is formed that presents stronger basicity than the starting hydrotalcite [67]. Then when gold is deposited, the results in Table 2, entry 6, show a lower TOF for gold on the mixed oxides than for the gold on hydrotalcite (entry 2). In spite of the acceptable activity of the Au/HTcalc (entry 6), the conversion achieved after 24 h of reaction is considerably lower than with Au/HT catalyst. As can be observed in Fig. 2, a strong deactivation occurs with this catalyst. This behavior can be attributed to the existence of strong basic sites on the support, which could promote the strong adsorption of the weak acidic diol giving the deactivation of the catalyst. In fact, when MgO was used as support, and despite its large surface area ($\geq 600 \text{ m}^2 \text{ g}^{-1}$), the average crystallite size of supported gold is larger and gives low activities and selectivities. It appears then

that some basicity of the support and high metal dispersion (small gold nanoparticles) would be positive for the reaction. Notice that when the reaction was carried out with the supports (CeO_2 and HT) without gold, the yields to product **3a** were much lower (Table 2, entries 7 and 8), whereas no products were detected in the absence of catalyst. Therefore, if one takes into account that the controlling step for the reaction is alcohol oxidation, it appears clear that smaller gold nanoparticles supported on carriers with mild basicity and carriers able to adsorb large amount of oxygen should be adequate catalyst for the one-pot two-step synthesis of quinoxalines.

3.3. Stability and reusability of Au/ CeO_2 and Au/HT catalysts

Catalyst recyclability was checked by performing successive reuses of the catalyst under the same reaction conditions. To do

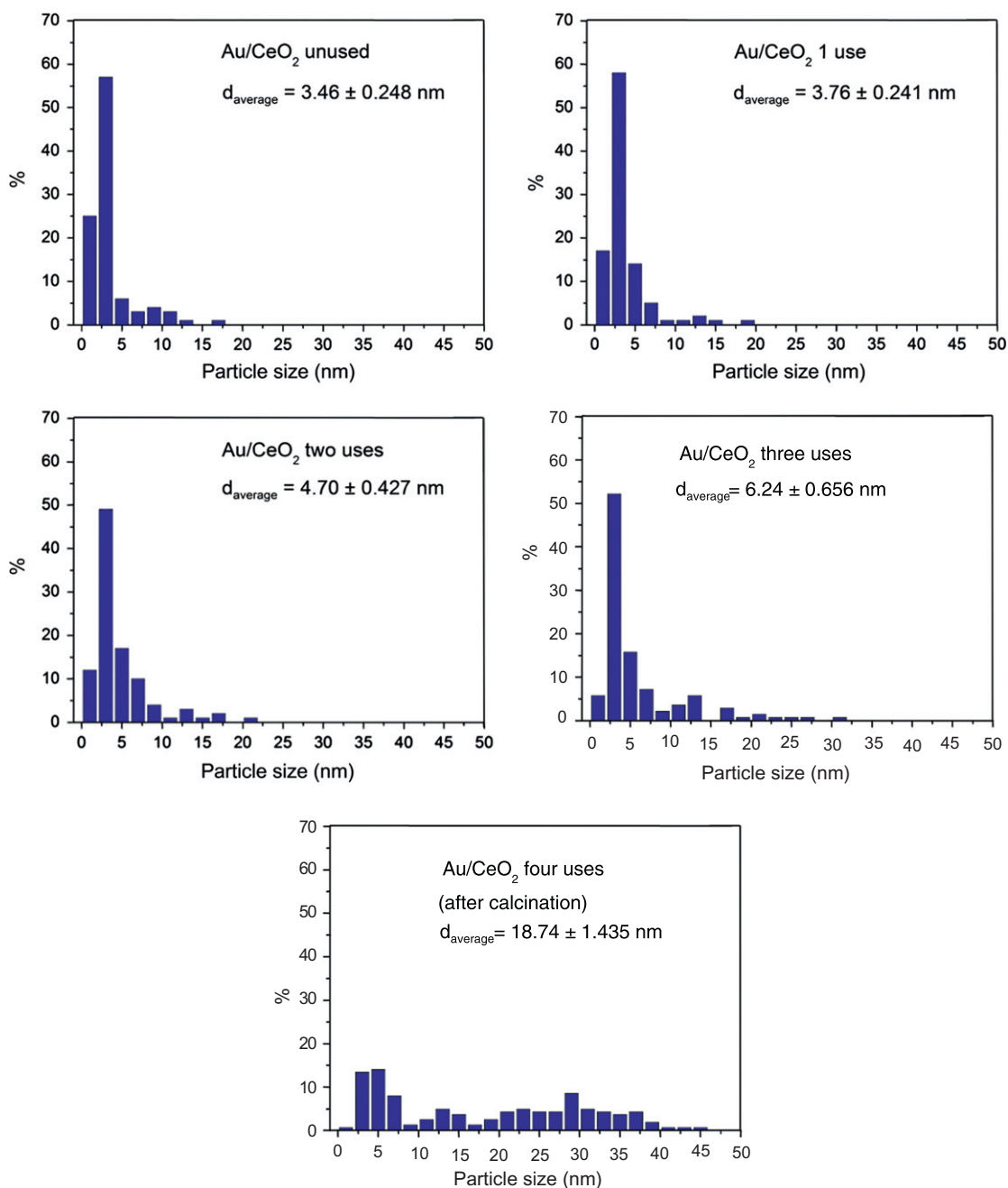


Fig. 6. Gold nanoparticle size of Au/ CeO_2 after several uses.

that, the catalyst recovered, as explained in the experimental section, was used in a subsequent run. The results of Au/CeO₂ catalyst recycling are shown in Figs. 3 and 4. As can be seen there, Au/CeO₂ catalyst slowly deactivates with use.

In order to check whether deactivation was due to gold leaching and the leached gold was the main responsible for activity, the reaction was performed under the same conditions, and after 2 h the gold catalyst was removed by filtration, being the reaction continued with the filtrate. Under these conditions, no further conversion was observed (Fig. 5). In addition, no traces of gold were detected in the reaction filtrate. Furthermore, the gold content in the used catalyst was determined by X-ray fluorescence, and no changes were detected with this technique after four runs. These results indicate that deactivation of the catalyst after four runs is not due to gold leaching from the support. A TG analysis of the used Au/CeO₂ sample showed that 5 wt% of organic material remains on the catalyst after the first use, which increases up to 14 wt% after the third use. Therefore, it may very well occur that the organic deposited on the catalyst surface could be the cause of catalyst deactivation. Then, in a new recycling experiment, after the third use, the catalyst was treated in air at 300 °C for 10 h. After calcination, the organic content of the catalyst was reduced from 14 to 3 wt%. When this catalyst was used again in the reaction, it was observed that, although some of the activity was recovered, the activity was still lower than for the fresh catalyst (see Fig. 3 and cycle 4 in Fig. 4). The lower activity of the regenerated catalyst could be explained by an increase in the size of gold nanoparticle due to metal agglomeration occurring during calcination. To check this possibility, the metal crystal size was determined by TEM for the used catalyst, and the results from Fig. 6 clearly show that crystal agglomeration occurs during calcination. Finally to address the deactivation issue, we have also considered a potential loss of activity due to the presence of carboxylic acids [68] which could be formed by deep oxidation of the diol and that act as poison for gold. To check that possibilities, an experiment was carried out in the presence of KOH to avoid acid deposition on the catalyst, but a significant decrease in the selectivity to 2-methylquinoxaline was observed (64% at full conversion). Therefore, we believe that catalyst deactivation during reaction mainly occurs by “coking,” but by burning off the organic deposits provided that metal synthesis is avoided. Therefore, catalyst regeneration for this process needs to be explored more deeply.

Similar results were obtained during the recycling of Au/HT catalyst (see Fig. 7), that is, the catalyst deactivates, but leaching of gold was not detected. However, catalyst calcination at 300 °C does not restore but further decreases activity (cycle 4, Fig. 8); this is probably due (see Fig. 9) to an increase in the basicity of the support due to the calcination treatment, which agrees with the results previously presented in Table 2, entry 6.

3.4. Optimization of reaction conditions: diamine/Au ratio, temperature, oxygen pressure, and gold average size

Taking into account activity, selectivity, regenerability, and performance of the catalyst, we have selected Au/CeO₂ as the catalyst to synthesize quinoxalines, and the influence of reaction conditions on conversion and selectivity has been studied. Firstly, the conversion to 2-methylquinoxaline with reaction time was followed using Au/CeO₂ and working at reactant-to-gold molar ratio of 100, 200, and 400 (see Table 3). The initial reaction rate is directly proportional to the concentration of the catalyst, and as can be observed in Table 3 (entries 1, 2, and 3), >95% conversion of **1a** can already be achieved with 1% molar catalyst loading.

The influence of the temperature (100 °C, 120 °C, 140 °C, and 160 °C) on the reaction rate, working at 1 mol% Au content, is shown in Table 3 (entries 3, 4, 5, and 6). As can be expected, when

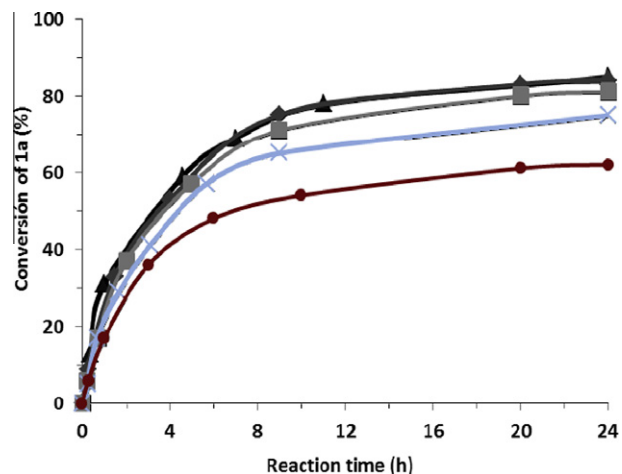


Fig. 7. Conversion kinetic plots of the oxidation-cyclization of **1a** with **2a** into **3a** under successive reuses of Au/HT: 1st use (▲), 2nd use (◆), 3rd use (■), 4th use (×) and 4th use after calcination (●) treatment with air at 300 °C for 10 h. Reaction conditions: **1a** (0.5 mmol), **2a** (0.6 mmol), diglyme (10.5 mmol), at 140 °C.

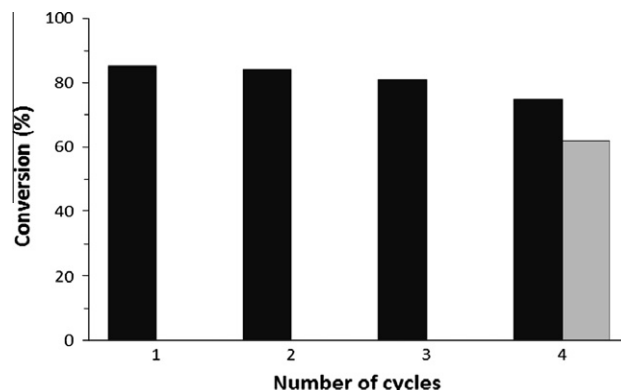


Fig. 8. Conversion of **1a** with successive reuses of Au/HT in the oxidation-cyclization of **1a** with **2a** after 24 h. In the fourth use, there are two bars because the bar on the right illustrates when the catalyst was used after previous treatment in air at 300 °C for 10 h. Reaction conditions: **1a** (0.5 mmol), **2a** (0.6 mmol), diglyme (10.5 mmol), Au/CeO₂ (4.5 wt%), **1a**/Au mol ratio = 100, at 140 °C.

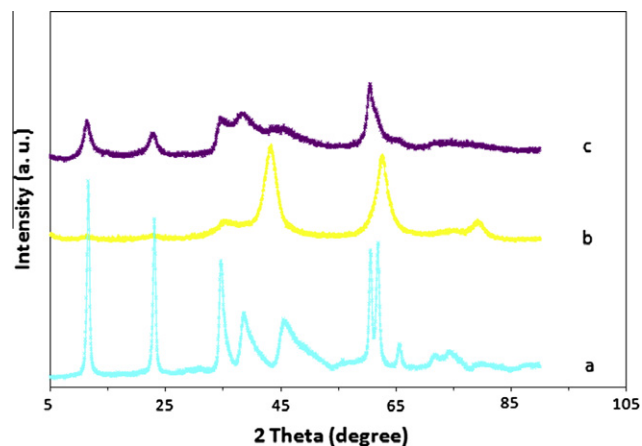


Fig. 9. XRD patterns of the catalyst Au/HT under different calcination treatment: (a) Au/HT, (b) Au/HT calcined at 300 °C, (c) Au/HT calcined at 450 °C.

increasing the temperature an increase in the reaction rate is observed, while selectivity to **3a** decreases at temperature higher than 140 °C owing to the oxidative cleavage of the glycol which

Table 3
Results of oxidation–cyclization process of **2a** with **1a** into **3a** using Au/CeO₂.^a

Entry	Temperature (°C)	1a/Au (mol ratio)	Time (h)	r_0^b (mmol h ⁻¹)	Conversion (mol%)	Selectivity to 3a ^c (mol%)
1	140	400	24	0.12	67	94
2	140	200	24	0.16	85	89
3	140	100	24	0.22	95	87
4	100	100	48	0.09	47	98
5	120	100	30	0.15	69	97
6	160	100	16	0.26	99	77
7	140 ^d	100	24	0.22	91	76
8	140 ^e	100	24	0.23	95	73
9	140 ^f	100	24	0.25	93	69

^a Reaction conditions: **1a** (0.5 mmol), **2a** (0.6 mmol), diglyme (10.5 mmol), Au/CeO₂ (4.5 wt%), **1a**/Au mol ratio = 100, at 140 °C.

^b Calculated as moles of converted **1a** divided by reaction time (0.5 h).

^c Selectivity values at 40% conversion. As main by-products, which complete molar balance, are the following: 2-methyl-1*H*-benzo[d]imidazole (**8**) and 1*H*-benzo[d]imidazole (**9**).

^d Experiment carried out bubbling O₂ into the reaction mixture at a constant flow rate of 0.30 mL s⁻¹.

^e Experiment carried out under air pressure of 3 bars.

^f Experiment carried out under oxygen pressure of 3 bars.

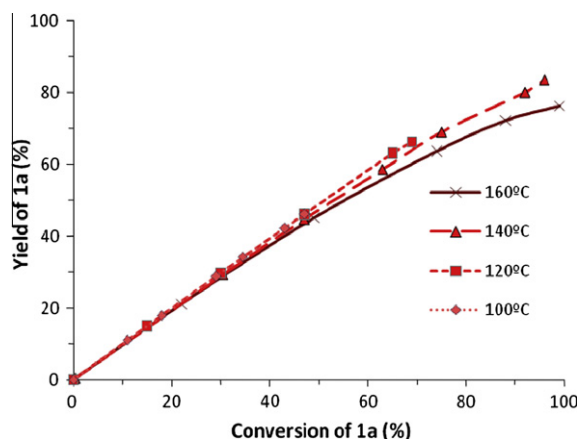


Fig. 10. Effect of temperature on **3g** selectivity in the oxidation–cyclization of **1a** with **2a** using Au/CeO₂. Reaction conditions: **1a** (0.5 mmol), **2a** (0.6 mmol), diglyme (10.5 mmol), Au/CeO₂ (4.5 wt%), **1a**/Au mol ratio = 100, at 140 °C.

is more favored when increasing the reaction temperature (see Fig. 10). Therefore, 140 °C was selected as an optimum reaction temperature.

The influence of oxygen partial pressure was studied by performing the reaction while continuously bubbling O₂ (Table 3, entry 7), or by working in a closed reaction system under 3 bars of air or O₂ (entries 8 and 9). The results obtained indicate that while the rate of the reaction does not increase when increasing oxygen partial pressure, the selectivity to 2-methylquinoxaline decreases due to an increase in the production of benzimidazole derivatives. This is due to the fact that at higher oxygen partial pressure, the oxidative cleavage of the glycol is favored (see Scheme 5).

Finally, the influence of the gold morphology on activity and selectivity has been studied. Then, the reaction of *o*-phenylenediamine with 1,2-propyleneglycol was performed using Au/CeO₂ with different gold average sizes (3.5, 4.0, 5.5, and 7.1 nm). In Fig. 11 is presented the initial rate of the reaction (obtained from the slope of the curve conversion versus reaction time at conversions below 15%), divided by the surface gold atoms versus the average gold crystallite size. The plot shows that the catalytic activity depends mainly on the percentage of gold atoms accessible. Further, the same figure shows that when the selectivity is plotted versus the average crystallite of gold size, it remains almost constant and only a small decrease is observed when increasing the gold crystallite size.

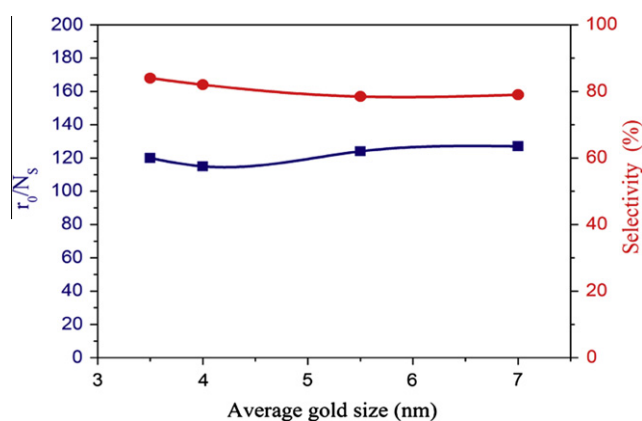


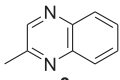
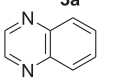
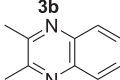
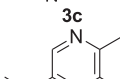
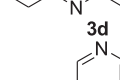
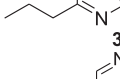
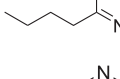
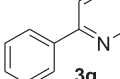
Fig. 11. Influence of average gold size of Au/CeO₂ catalyst on initial activity per gold surface atom (■) and on selectivity to **3a** (●). Reaction conditions: **1a** (0.5 mmol), **2a** (0.6 mmol), diglyme (10.5 mmol), Au/CeO₂, **1a**/Au mol ratio = 100, at 140 °C.

3.5. Scope of the reaction

Under optimized reaction conditions, we have analyzed the possibility to perform the one-pot, two-step preparation of quinoxaline derivatives with Au/CeO₂ starting from several diols (1,2-ethanediol **2b**, 2,3-butanediol **2c**, 1,2-butanediol **2d**, 1,2-pentanediol **2e**, 1,2-hexanediol **2f**, 1-phenylethane-1,2-diol **2g**, and *m*-hydrobenzoin **2h**) and **1a**, and the results are given in Table 4. As can be seen there, conversion and selectivity to the corresponding quinoxalines were excellent except in the case of diols with aromatic substituent (**2g** and **2h**), which were more prone to undergo the oxidative cleavage.

The influence of different substituents in position 4 of 1,2-phenylenediamine (4-nitrobenzene-1,2-diamine **1b**, 4-chlorobenzene-1,2-diamine **1c**, 3,4-diaminobenzonitrile **1d**, 4-methylbenzene-1,2-diamine **1e**, naphthalene-2,3-diamine **1f**, 4-methoxybenzene-1,2-diamine **1g**) on the reaction rate and product selectivity for the oxidation–cyclization process of 1,2-ethanediol (**2b**) was studied in the presence of Au/CeO₂. As can be seen in Table 5, good yields to quinoxaline derivatives are obtained in all cases. However, when electron withdrawing substituent, such as nitro, chloride, or nitrile groups, is present, quinoxaline derivative yields are lower with respect to 1,2-phenylenediamine (Table 5, entries 1–4), or with respect to phenylenediamine molecules with electron-donating substituents like methyl, (–CH₂)₄ or methoxy groups (Table 5, entries 5–7). Similar results have been described in the literature

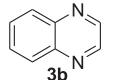
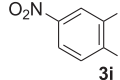
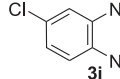
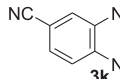
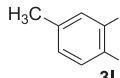
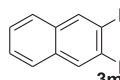
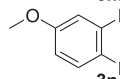
Table 4
Influence of the diol substituents on the oxidation–cyclization process with **1a** using Au/CeO₂.^a

Entry	Diol	Product	Conversion (mol%)	Selectivity to 3a–h ^b (mol%)	Yield (mol%)
1			96	87	84
2			99	92	91
3			98	89	87
4			96	85	81
5			94	86	80
6			99	82	81
7			97	72	70
8			99	35	35

^a Reaction conditions: **1a** (0.5 mmol), diol (0.6 mmol), diglyme (10.5 mmol), Au/CeO₂ (4.5 wt%), **1a**/Au mol ratio = 100, at 140 °C, 24 h.

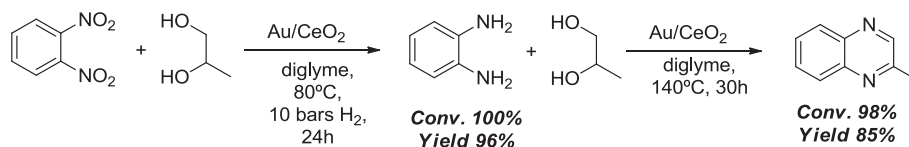
^b Selectivity values at 90% conversion. As main by-products, which complete molar balance, are the correspondents benzimidazoles produced from the oxidative cleavage of the diol (**8** and **9**).

Table 5
Influence of the 1,2-phenylenediamine substituent in position 4 on the oxidation–cyclization process of diamine with **2b** using Au/CeO₂.^a

Entry	Reactant	Product	Conversion (mol%)	Selectivity to 3a, 3i–n ^b (mol%)	Yield (mol%)
1			99	92	91
2			90	78	70
3			92	80	73
4			91	83	75
5			97	88	86
6			95	84	81
7			99	89	88

^a Reaction conditions: diamine (0.5 mmol), **2b** (0.6 mmol), diglyme (10.5 mmol), Au/CeO₂ (4.5 wt%), **1a**/Au mol ratio = 100, at 140 °C, 24 h.

^b Selectivity values at 90% conversion. As main by-product, which complete molar balance, is the 1H-benzo[d]imidazole substituted at position 6 (**9**).



Scheme 7. Synthesis of 2-methylquinoxaline by one-pot reaction between 1,2-dinitrobenzene **15** and **2a** using Au/CeO₂, in 1.5 mL diglyme and mol ratio 1a/Au = 100.

for the reaction between α -hydroxycarbonyl compounds and 1,2-phenylenediamine derivatives [31,35,37].

3.6. One-pot three-step synthesis of quinoxalines

Owing to the success of Au/CeO₂ for catalyzing the oxidation–cyclization of 1,2-diamines with 1,2-diols, and taking into account the gold ability for the chemoselective reduction of nitro to amino groups [54,69–71], we have attempted a one-pot three-step process which involves the reaction between 1,2-dinitrobenzene **15** and 1,2-propanediol **2a** to achieve the one-pot synthesis of 2-methylquinoxaline as shown in Scheme 7. Firstly, the reduction of nitro to amino is performed at 10 bars of H₂ and 80 °C of temperature. After that, the system is depressurized and flashed out with N₂, and the reaction is continued at 140 °C and atmospheric pressure in the presence of air. The results obtained (see Scheme 7) indicate that the reduction step is almost quantitative, with complete conversion and selectivity to 1,2-phenylenediamine higher than 95%. The following oxidation–cyclization step was performed with excellent results (98% conversion and 85% yield to **3a**). Therefore, Au/CeO₂ is a good bifunctional catalyst able to perform the one-pot three-step reaction between 1,2-dinitrobenzene and vicinal diols derivatives to give the respective quinoxaline.

4. Conclusions

Au/HT and Au/CeO₂ are excellent catalysts for the synthesis of quinoxaline derivatives of 1,2-propanediol followed by cyclocondensation with 1,2-phenylenediamine under base-free conditions, at mild temperature and using air at atmospheric pressure as oxidant. The reaction network has been established being the diol **2** firstly oxidized to α -hydroxycarbonyl compound **4** (which is the controlling step) and subsequently to the dicarbonyl compound **5**. Both compounds condensate with 1,2-phenylenediamine giving the quinoxaline **3**. The oxidative cleavage of the diol is a competitive reaction which is enhanced by higher temperatures and pressures of the oxidant (air or oxygen). Au/CeO₂ can be easily recovered and reused with a small loss of activity that can be partially restored by removing the adsorbed organic material by a calcination treatment. This calcination treatment should be optimized to avoid or decrease metal sintering. The regenerated catalyst maintains high selectivity toward 2-methylquinoxaline. With Au/HT, it is more difficult to recover the initial activity after some uses.

The catalytic process presented here has been extended to different substrates (diols and 1,2-diamines derivatives), achieving good yields of the corresponding quinoxalines. Finally, Au/CeO₂ allows to carry out the one-pot three-step synthesis of 2-methylquinoxaline starting from 1,2-dinitrobenzene with an excellent global yield of 83%.

Acknowledgments

The authors wish to acknowledge the Spanish Ministry of Education and Science for the financial support in the projects Consolider-Ingenio 2010 and CTQ-2011-27550. Generalitat Valenciana is also thanked for funding through the Prometeo

program. S.M.S thanks Spanish Ministry of Education and Science for FPI fellowships.

References

- [1] A. Corma, S. Iborra, A. Velty, *Chem. Rev.* 107 (2007) 2411.
- [2] G.W. Huber, S. Iborra, A. Corma, *Chem. Rev.* 106 (2006) 4044.
- [3] P. Gallezot, *Green Chem.* 9 (2007) 295.
- [4] C.H. Christensen, J. Rass-Hansen, C.C. Marsden, E. Taarning, K. Egeblad, *Chem. Sus. Chem.* 1 (2008) 283.
- [5] J. van Haveren, E.L. Scott, J. Sanders, *Biofuels Bioprod. Bioref.* 2 (2008) 41.
- [6] H. Roper, *Starch-Starke* 54 (2002) 89.
- [7] F.W. Lichtenthaler, *Chem. Res.* 35 (2002) 728.
- [8] F.W. Lichtenthaler, S.C.R. Peters, *Chimie* 7 (2004) 65.
- [9] F.W. Lichtenthaler, *Carbohydr. Res.* 113 (1998) 69.
- [10] M.J. Climent, A. Corma, P. De Frutos, S. Iborra, M. Noy, A. Velty, P. Concepción, *J. Catal.* 269 (2010) 140.
- [11] K.M. Rapp, J. Daub, K.M. Rapp, J. Daub, in: Hrsrg, S. Warwel, G. Wulff (Eds.), *Nachwachsende Rohstoffe: Perspektiven für die Chemie*, VCH, Weinheim, 1993, p. 183.
- [12] V. Lehr, M. Sarlea, L. Ott, H. Vogel, *Catal. Today* 121 (2007) 121.
- [13] M. Pagliaro, R. Ciriminna, H. Kimura, M. Rossi, C.D. Pina, *Angew. Chem. Int. Ed.* 46 (2007) 4434.
- [14] S.H.C. Zhou, J.N. Beltramini, Y.X. Fan, G.Q.M. Lu, *Chem. Soc. Rev.* 37 (2008) 527.
- [15] S.T. Hazeldine, L. Polin, J. Kushner, J. Paluch, K. White, M. Edelstein, E. Palomino, T.H. Corbett, J.P. Horwitz, *J. Med. Chem.* 44 (2001) 1758.
- [16] F. Rong, S. Chow, S. Yan, G. Larson, Z. Hong, J. Wu, *Bioorg. Med. Chem. Lett.* 17 (2007) 1663.
- [17] A. Jaso, B. Zarranz, I. Aldana, A. Monge, *J. Med. Chem.* 48 (2005) 2019.
- [18] R.A. Smits, H.D. Lim, A. Hanzer, O.P. Zuidelverd, E. Guaita, M. Adami, G. Coruzzi, R. Leurs, I.J.P. De Esch, *J. Med. Chem.* 51 (2008) 2457.
- [19] G.W.H. Cheeseman, E.S.G. Werstiuk, *Adv. Heterocycl. Chem.* 22 (1978) 367.
- [20] K. Yb, K. Yh, P. Jy, K. Sk, *Bioorg. Med. Chem. Lett.* 14 (2004) 541.
- [21] X. Hui, J. Desrivot, C. Bories, P.M. Loiseau, X. Franck, R. Hocquemiller, B. Fidadere, *Bioorg. Med. Chem. Lett.* 16 (2006) 815.
- [22] G. Sakata, K. Makino, Y. Karasawa, *Heterocycles* 27 (1988) 2481.
- [23] E.D. Brock, D.M. Lewis, T.I. Yousaf, H.H. Harper, *The Procter and Gamble Company*, USA, 1999, p. WO9951688.
- [24] J.L. Sessler, H. Maeda, T. Mizuno, V.M. Lynch, H.J. Furuta, *Am. Chem. Soc.* 124 (2002) 13474.
- [25] K.R.J. Thomas, M. Velusamy, J.T. Lin, C.-H. Chuen, Y.-T. Tao, *Chem. Mater.* 17 (2005) 1860.
- [26] S. Dailey, W.J. Feast, R.J. Peace, I.C. Sage, S. Till, E.L. Wood, *J. Mater. Chem.* 11 (2001) 2238.
- [27] M.J. Crossley, L.A. Johnston, *Chem. Commun.* (2002) 1122.
- [28] O. Sascha, F. Rudiger, *Synlett* (2004) 1509.
- [29] D.J. Brown, *Quinoxalines supplements II*, in: E.C. Taylor, P. Wipf (Eds.), *The Chemistry of Heterocyclic Compounds*, John Wiley & Sons, New Jersey, 2004.
- [30] R.S. Bhosale, S.R. Sarda, S.S. Andhapure, W.N. Jadhav, S.R. Bhusare, R.P. Pawar, *Tetrahedron Lett.* 46 (2005) 7183.
- [31] Z. Zhao, D.D. Wisnoski, S.E. Wolkenberg, W.H. Leister, Y. Wang, C.W. Lindsley, *Tetrahedron Lett.* 45 (2004) 4873.
- [32] S.V. More, M.N.V. Sastry, C.F. Yao, *Green Chem.* 8 (2006) 91.
- [33] C. Srinivas, C.N.S.S.P. Kumar, V.J. Rao, S. Palaniappan, *J. Mol. Catal. A: Chem.* 256 (2007) 227.
- [34] D. Aparicio, O.A. Attanasi, P. Filippone, R. Ignacio, S. Lillini, F. Mantellini, F. Palacios, J.M. De los Santos, *J. Org. Chem.* 71 (2006) 5897.
- [35] S.A. Raw, C.D. Wilfred, R.J.K. Taylor, *Org. Biomol. Chem.* 2 (2004) 788.
- [36] S.Y. Kim, K.H. Park, Y.K. Chung, *Chem. Commun.* (2005) 1321.
- [37] R.S. Robinson, R.J.K. Taylor, *Synlett* (2005) 1003.
- [38] S. Sithambaram, Y. Ding, W. Li, X. Shen, F. Gaenzler, S.L. Suib, *Green Chem.* 10 (2008) 1029.
- [39] S.K. Singh, P. Gupta, S. Duggineni, B. Kundu, *Synlett* 14 (2003) 2147.
- [40] S. Antoniotti, E. Duñach, *Tetrahedron Lett.* 43 (2002) 3971.
- [41] C.S. Cho, S.G. Oh, *Tetrahedron Lett.* 47 (2006) 5633.
- [42] A. Corma, *Catal. Rev.* 46 (2004) 369.
- [43] M.J. Climent, A. Corma, S. Iborra, *Chem. Sus. Chem.* 2 (2009) 500.
- [44] M.J. Climent, A. Corma, S. Iborra, *Chem. Rev.* 111 (2011) 1072.
- [45] M.J. Climent, A. Corma, S. Iborra, *RSC Adv.* 2 (2012) 16.
- [46] D. Venu Gopal, M. Subrahmanyam, *Catal. Commun.* 2 (2001) 219.
- [47] K.V. Rao, M. Subba, M. Subrahmanyam, *Chem. Lett.* 2 (2002) 234.
- [48] T. Mallat, A. Baiker, *Catal. Today* 19 (1994) 247.
- [49] S.-I. Murahashi, N. Komiya, in: S.-I. Murahashi (Ed.), *Ruthenium in Organic Synthesis*, Wiley-VCH, Weinheim, 2004, p. 53.

- [50] A. Abad, P. Concepcion, A. Corma, H. Garcia, *Angew. Chem. Int. Ed.* 44 (2005) 4066.
- [51] A. Abad, C. Almela, A. Corma, H. Garcia, *Chem. Commun.* 30 (2006) 3178.
- [52] R. Juárez, A. Corma, H. Garcia, *Green Chem.* 11 (2009) 949.
- [53] F. Cavani, A. Trifiró, A. Vaccari, *Catal. Today* 11 (1991) 173.
- [54] M.J. Climent, A. Corma, S. Iborra, L. Santos, *Chem. Eur. J.* 15 (2009) 8834.
- [55] R.G. Jacob, L.G. Dutra, C.S. Radatz, S.R. Mendes, G. Perin, E.J. Lenardao, *Tetrahedron Lett.* 50 (2009) 1495.
- [56] R. Van Hardeveld, F. Hartog, *Surf. Sci.* 15 (1969) 189.
- [57] R.E. Benfield, *J. Chem. Soc. Faraday Trans.* 88 (1992) 1107.
- [58] A. Corma, H. García, *Nanoparticles Catal.* (2008) 389.
- [59] L. Zhang, S.A. Kozmin, *J. Am. Chem. Soc.* 126 (2004) 11806.
- [60] Q. Fu, H. Saltsburg, M. Flytzani-Stephanopoulos, *Science* 301 (2003) 935.
- [61] J. Guzman, S. Carrettin, A. Corma, *J. Am. Chem. Soc.* 127 (2005) 3286.
- [62] J. Guzman, S. Carrettin, J.C. Fierro-González, L. Hao, B.C. Gates, A. Corma, *Ang. Chem. Int. Ed.* 44 (2005) 4778.
- [63] T. Mitsudome, A. Noujima, T. Mizugaki, K. Jitsukawa, K. Kaneda, *Green Chem.* 11 (2009) 793.
- [64] T. Mitsudome, Y. Mikami, H. Funai, T. Mizugaki, K. Jitsukawa, K. Kaneda, *Angew. Chem. Int. Ed.* 47 (2008) 138.
- [65] T. Mitsudome, Y. Mikami, K. Ebata, T. Mizugaki, K. Jitsukawa, K. Kaneda, *Chem. Commun.* (2008) 4804.
- [66] K. Ebitani, K. Motokura, T. Mizugaki, K. Kaneda, *Angew. Chem. Int. Ed.* 44 (2005) 3423.
- [67] F. Rey, V. Fornés, *J. Chem. Soc. Faraday Trans.* 88 (1992) 2223.
- [68] I.S. Nielsen, E. Taarning, K. Egeblad, R. Madsen, C.H. Christensen, *Catal. Lett.* 116 (2007) 35.
- [69] Y. Azizi, C. Petit, V. Pitchon, *J. Catal.* 256 (2008) 338.
- [70] A. Corma, C. González-Arellano, M. Iglesias, F. Sánchez, *Appl. Catal. A: Gen.* 356 (2009) 99.
- [71] A. Corma, P. Serna, *Science* 313 (2006) 332.